may be a fluxional molecule. The limited solubility of the complex precluded ^{1}H NMR spectra at lower temperatures.
(48) G. M. Brown, T. R. Weaver, F. R. Keene, and T. J. Meyer, *Inorg. Chem.*, **15**, 190 (1976).
(49) S. Piekarski and R. N. Adams in "Physical Methods of Chemistry", Part 11A, "Electrochemical Methods", Weissberger and Rossiter, Ed., Wiley-Interscience, New York, N.Y., 1971.
(50) E. R. Brown and R. F. Large in ref 49.
(51) G. Ciantelli and F. Pantani, *Ric. Sci.*, **38**, 706 (1968).
(52) J. B. Headridge, "Electrochemical Techniques for Inorganic Chemists", Academic Press, New York, N.Y., 1969, p 47.
(53) N. E. Tokel, R. E. Hemingway, and A. J. Bard, *J. Am. Chem. Soc.*, **95**, 6582 (1973).
(54) G. M. Brown, R. W. Callahan, and T. J. Meyer, *Inorg. Chem.*, **14**, 1915 (1975).
(55) R. R. Schrock, B. F. G. Johnson, and J. Lewis, *J. Chem. Soc., Dalton Trans.*, 951 (1974).
(56) K. F. Purcell and R. S. Drago, *J. Am. Chem. Soc.*, **88**, 919 (1966).
(57) F. A. Cotton and J. Zingales, *J. Am. Chem. Soc.*, **83**, 351 (1961).
(58) K. F. Purcell, *J. Am. Chem. Soc.*, **89**, 247 (1967).

Structure and Stereodynamic Behavior of (1,2-Diazine)decacarbonyl Triangulotriruthenium. Evidence for Hidden Processes in Fluxional Molecules

F. Albert Cotton,* Brian E. Hanson, and Jackie D. Jamerson

Contribution from the Department of Chemistry, Texas A&M University, College Station, Texas 77843. *Received February 23, 1977*

Abstract: A derivative of $Ru_3(CO)_{12}$, in which two cis axial CO ligands are replaced by the bidentate ligand 1,2-diazene (pyridazine), has been prepared and characterized structurally and stereodynamically by x-ray crystallography and ^{13}C NMR. The arrangement of the equatorial (in-plane) CO groups is changed from all terminal as in $Ru_3(CO)_{12}$ and now consists of three terminal ones and three slightly unsymmetrical bridging ones. Crystal data: space group, $P\bar{1}$; $a = 9.272$ (2) Å, $b = 13.727$ (2) Å, $c = 8.973$ (1) Å, $\alpha = 103.44$ (1)°, $\beta = 120.53$ (1)°, $\gamma = 90.01$ (1)°, $V = 947.1$ (3) Å^3, $Z = 2$. Using 2304 data with $I > \sigma(I)$, anisotropic refinement converged with $R_1 = 0.024$ and $R_2 = 0.039$. A ^{13}C NMR study over the temperature range −156 to 75 °C reveals three distinct phases of fluxionality the cumulative effect of which is to transform the seven-line slow exchange spectrum (−156 °C) that is consistent with the crystal structure into a spectrum (75 °C) consisting of only one sharp line. Phase one, which alters the spectrum between −156 and about −90 °C, consists in the equivalencing of the six equatorial CO groups. Phase two, whose effects are observed mainly from about −115 to −80 °C, involves a process that is difficult to define with certainty, but appears to introduce one axial CO group into the averaging process seen in phase one. Phase three, whose effects become evident above about −30 °C, results in collapse and merging of the three separate lines of relative intensities 7:2:1 into a single line. Dynamic processes capable of accounting for these spectral changes are suggested and discussed.

The stereodynamic behavior of $M_3(CO)_{12}$ molecules (M = Fe, Ru, Os) and their multitudinous derivatives, many of which are of special interest with regard to catalysis,[1] is one of the focal points in current research on fluxionality in polynuclear organometallic and metal carbonyl type molecules. Despite a number of significant discoveries, our factual knowledge of the stereodynamic capabilities of these systems remains very fragmentary, and our comprehension of the structural and mechanistic principles underlying the observations is correspondingly incomplete. We report and analyze here an investigation designed to penetrate the superficial simplicity of the situation regarding the parent carbonyls themselves by using a judiciously designed substitution product. This work provides the first direct observation of limited and "unperceived" (in the sense that we have previously[2] defined that term) scrambling processes for some of the CO groups. The certain knowledge that one of these processes takes place has an important bearing on how one evaluates the recent proposal of Johnson[3] for "truly concerted" scrambling in $Fe_3(CO)_{12}$ and related species, an issue we shall return to later in this paper.

The crystal structures of the three parent $M_3(CO)_{12}$ molecules are known. $Fe_3(CO)_{12}$ has the least symmetrical structure, **1**, in the crystal,[4] while $Ru_3(CO)_{12}$[5] and $Os_3(CO)_{12}$[6] have the D_{3h} structure **2** in which there are no bridging CO groups. It has been shown that for $Fe_3(CO)_{12}$ the replacement of some CO groups by phosphorus or sulfur ligands causes the degree of asymmetry in the bridging system to vary greatly, from one case in which the bridges are essentially symmetrical to another in which they are only incipient.[7] This observation, coupled with the fact that $Fe_3(CO)_{12}$ undergoes rapid carbonyl scrambling (even at −150 °C[8]), led us to propose, first in 1974[4b] and later in more detail,[8] the mechanism shown in Scheme I for total scrambling of CO groups in $Fe_3(CO)_{12}$. It was also suggested[4a,7,8] that the entire potential energy hypersurface traversed by the entire set of configurations of the types shown in Scheme I as they interconvert is so flat that a continuous range of intermediate dispositions of CO groups is present in solution. In this way the very unusual and previously unexplained infrared spectrum of $Fe_3(CO)_{12}$ became understandable for the first time.[8]

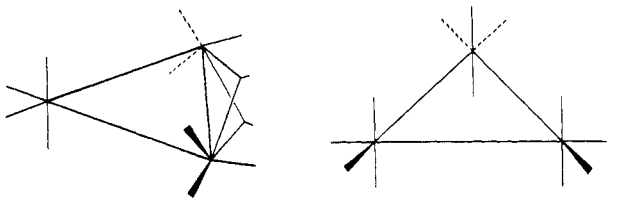

1 **2**

It was, of course, perfectly obvious that Scheme I could equally well afford an explanation for CO scrambling, should it be observed, in $Ru_3(CO)_{12}$ and $Os_3(CO)_{12}$. However, it was not until later that ^{13}C NMR spectra were published for these molecules.[9-12] It should be noted that for $Ru_3(CO)_{12}$ and $Os_3(CO)_{12}$ infrared spectra show, straightforwardly, that the structures in solution are the same as those in the crystalline compounds. After one report that $Ru_3(CO)_{12}$ at room temperature has two resonances,[9] followed by another[10] that even at −50 °C there is only one, a third report[11] showed that even

Scheme I

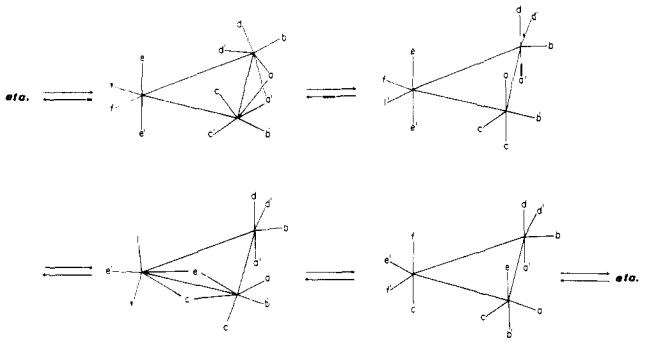

Scheme II

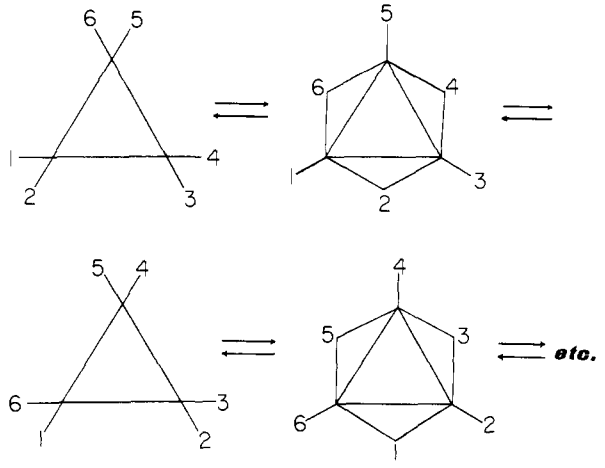

Scheme III

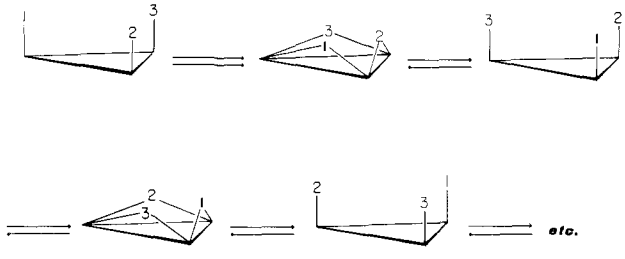

at −100 °C there is only one signal, and also proposed a specific impurity to account for the additional signal erroneously reported in the first case. Thus, it seems clear (barring the unlikely event of accidental degeneracy of axial and equatorial resonances) that even at −100 °C $Ru_3(CO)_{12}$ is rapidly executing one or more intramolecular rearrangements that, at the very least, cause localized interchange of axial and equatorial CO groups, and perhaps also internuclear scrambling. For $Os_3(CO)_{12}$ it has been reported independently by two groups[10,11] that at and below room temperature there are two resonances of equal intensity, while above 90 °C there is only a single resonance at the proper average position; the coalescence temperature is around 75 °C.

There are three ways to account for the observation of a spectrum with only one signal for $Ru_3(CO)_{12}$ and $Os_3(CO)_{12}$. One general possibility is that CO groups are scrambled over the entire M_3 core (i.e., scrambled internuclearly) in some way that incorporates axial-equatorial (ax/eq) exchange. It is important to keep in mind that *only* ax/eq exchange, whether localized or delocalized, is required to explain the observed spectra. One such process, as noted above, is that in Scheme I. Others can be envisioned, but this one has the special appeal of employing an intermediate that is actually the observed structure in the homologous $Fe_3(CO)_{12}$. The other two ways to account for the observed ax/eq exchange are the two possible forms of localized ax/eq exchange, one involving both ax and both eq ligands exchanging simultaneously (a possibility already mentioned in the literature[10]) and the other a sequence of 1 for 1 exchanges (a possibility not previously mentioned).

There is, finally, the possibility—and this is the focus of interest in this paper—that still other processes might occur that are unperceived and are, indeed, *unperceivable* by simple observation of line shape changes in the highly symmetrical molecules $M_3(CO)_{12}$, because they lead to no exchange of nuclei between sites characterized by different chemical shifts. Two examples of such processes are cycling of either axial or equatorial CO groups over the triangular M_3 core. These are illustrated in Schemes II and III. Evidence for the occurrence of such processes might, in principle, be obtained by observing C-C and/or M-C coupling, and changes therein. In practice, however, such observations have not been, and do not seem likely to be, helpful. For Ru and Os there are no available nuclides with proper characteristics (i.e., nuclear properties and abundance). It also appears (as will be shown) that coupling between mutually cis CO ligands (i.e., between geminal axial and equatorial ones, in the context appropriate here) is vanishingly small.

One way to open up new avenues for obtaining information is to introduce judiciously chosen substituents, so as to "complicate" the problem in an *informative* way. We shall report and discuss an example of such an experiment here. A partial report of this work has already appeared in preliminary form.[2] Using a suitable ligand, 1,2-diazine, we have replaced two adjacent axial CO groups, thus reducing the symmetry of the molecule. The structure of the product, $Ru_3(CO)_{10}C_4H_4N_2$, has been established x-ray crystallographically and the dynamic properties of the molecule have been investigated by ^{13}C NMR spectroscopy from −156 to 75 °C.

Experimental Section

All operations were performed in an atmosphere of dry nitrogen. Solvents were dried over potassium benzophenone and were distilled under nitrogen just prior to use. Pyridazine (97%) was purchased from Aldrich Chemical Co. and ruthenium carbonyl was purchased from Strem Chemical Co. Elemental analyses were performed by Galbraith Laboratories.

Synthesis of $(C_4H_4N_2)Ru_3(CO)_{10}$. Triruthenium dodecacarbonyl (0.62 g, 0.97 mmol) was dissolved in 60 mL of THF and then 0.073 mL (0.080 g, 1.0 mmol) of pyridazine was added. The resulting solution was warmed to ca. 50 °C for 24 h. The color of the reaction solution changed from orange to deep maroon. The reaction solution was concentrated under vacuum, and then chromatographed on Florisil. Elution was begun with hexane to remove unreacted $Ru_3(CO)_{12}$, and continued with THF. The eluate was then taken to dryness under vacuum to yield 0.42 g of product (65% yield). Crystals suitable for x-ray crystallography were obtained from a THF-hexane solution at −20 °C.

Anal. Calcd for $C_{14}H_4N_2O_{10}Ru_3$: C, 25.36; H, 0.60; N, 4.23. Found: C, 25.5; H, 0.57; N, 3.99.

The infrared spectrum in THF solution has a broad band, which is probably an unresolved envelope of two or more bands, centered at 1820 cm^{-1}, and a number of peaks in the terminal region at 2083 (m), 2035 (m), 2015 (s), 2003 (m), 1998 (s), and 1964 cm^{-1} (vb), the last one being probably an unresolved doublet.

X-Ray Data Collection. A maroon crystal of $(C_4H_4N_2)Ru_3(CO)_{10}$ measuring approximately 0.21 × 0.23 × 0.30 mm was sealed in a glass capillary. All data were collected at 21 ± 2 °C on a Syntex $P\bar{1}$ automated diffractometer using Mo Kα radiation monochromatized with a graphite crystal in the incident beam.

The automatic centering and autoindexing procedures followed have been described;[13] a triclinic space group was indicated, and $P\bar{1}$ was assumed. The principal crystallographic data are a = 9.272 (2) Å, b = 13.727 (2) Å, c = 8.973 (1) Å, α = 103.44 (1)°, β = 120.53

Table I. Positional and Thermal Parameters for $(C_4H_4N_2)Ru_3(CO)_{10}$[a,b] and Their Estimated Standard Deviations

Atom	x	y	z	β_{11}	β_{22}	β_{33}	β_{12}	β_{13}	β_{23}
Ru1	0.43341 (4)	0.31569 (3)	0.14661 (4)	0.01175 (5)	0.00315 (2)	0.01093 (5)	0.00138 (5)	0.01128 (7)	0.00156 (5)
Ru2	0.23871 (4)	0.12948 (3)	−0.00442 (4)	0.01232 (5)	0.00294 (2)	0.01340 (5)	0.00231 (5)	0.01261 (7)	0.00410 (5)
Ru3	0.08082 (4)	0.30043 (3)	−0.11100 (4)	0.01298 (5)	0.00396 (2)	0.01195 (5)	0.00541 (5)	0.01211 (7)	0.00504 (5)
O1	0.3967 (5)	0.3933 (3)	0.4672 (4)	0.0220 (5)	0.0078 (3)	0.0172 (5)	0.0027 (7)	0.0228 (7)	0.0023 (6)
O2	0.7833 (5)	0.4401 (4)	0.3501 (5)	0.0188 (6)	0.0118 (4)	0.0251 (7)	−0.0087 (8)	0.0218 (9)	−0.0030 (9)
O3	0.1280 (5)	0.1284 (3)	0.2578 (4)	0.0218 (5)	0.0089 (3)	0.0259 (5)	0.0036 (7)	0.0292 (7)	0.0135 (6)
O4	0.2549 (5)	−0.0967 (3)	−0.0664 (5)	0.0260 (7)	0.0040 (2)	0.0382 (9)	0.0060 (7)	0.0285 (11)	0.0096 (7)
O5	0.1162 (6)	0.2751 (4)	−0.4379 (5)	0.0416 (8)	0.0134 (3)	0.0225 (6)	0.0260 (9)	0.0422 (9)	0.0166 (7)
O6	−0.2144 (5)	0.4000 (3)	−0.3067 (5)	0.0261 (7)	0.0127 (3)	0.0259 (7)	0.0239 (7)	0.0216 (11)	0.0185 (7)
O7	−0.0093 (5)	0.3407 (3)	0.1823 (5)	0.0281 (6)	0.0113 (3)	0.0286 (6)	0.0145 (8)	0.0403 (8)	0.0131 (8)
O8	0.5885 (4)	0.1515 (3)	0.3471 (4)	0.0184 (6)	0.0063 (2)	0.0149 (5)	0.0069 (6)	0.0082 (8)	0.0083 (5)
O9	−0.1400 (5)	0.0889 (3)	−0.3037 (5)	0.0160 (6)	0.0056 (2)	0.0263 (8)	−0.0005 (7)	0.0026 (12)	0.0041 (7)
O10	0.3075 (5)	0.5062 (3)	0.0222 (5)	0.0253 (7)	0.0040 (2)	0.0301 (7)	0.0034 (6)	0.0233 (10)	0.0096 (5)
N1	0.4516 (4)	0.2373 (3)	−0.0773 (4)	0.0150 (5)	0.0030 (2)	0.0125 (5)	0.0026 (5)	0.0163 (7)	0.0024 (5)
N2	0.3538 (4)	0.1457 (3)	−0.1529 (4)	0.0132 (5)	0.0027 (2)	0.0142 (5)	0.0041 (5)	0.0137 (7)	0.0036 (5)
C1	0.4092 (5)	0.3664 (3)	0.3343 (5)	0.0122 (6)	0.0041 (3)	0.0135 (7)	0.0011 (7)	0.0103 (10)	0.0012 (7)
C2	0.6539 (6)	0.3930 (4)	0.2726 (6)	0.0152 (7)	0.0062 (3)	0.0146 (7)	−0.0008 (8)	0.0157 (10)	0.0004 (8)
C3	0.1660 (6)	0.1275 (3)	0.1542 (6)	0.0140 (6)	0.0044 (3)	0.0170 (7)	0.0029 (7)	0.0164 (9)	0.0068 (7)
C4	0.2463 (6)	−0.0120 (4)	−0.0453 (6)	0.0114 (6)	0.0045 (3)	0.0202 (8)	0.0031 (7)	0.0129 (10)	0.0074 (7)
C5	0.1090 (6)	0.2816 (4)	−0.3158 (6)	0.0210 (7)	0.0067 (3)	0.0141 (7)	0.0109 (8)	0.0192 (10)	0.0063 (8)
C6	−0.1015 (6)	0.3672 (4)	−0.2352 (6)	0.0162 (7)	0.0066 (3)	0.0159 (7)	0.0066 (8)	0.0167 (10)	0.0073 (8)
C7	0.0301 (6)	0.3264 (4)	0.0771 (6)	0.0156 (7)	0.0059 (3)	0.0183 (7)	0.0073 (8)	0.0188 (10)	0.0073 (8)
C8	0.4923 (6)	0.1824 (4)	0.2290 (5)	0.0138 (6)	0.0045 (3)	0.0119 (6)	0.0033 (7)	0.0128 (9)	0.0028 (7)
C9	−0.0115 (6)	0.1384 (4)	−0.2002 (6)	0.0157 (7)	0.0045 (3)	0.0148 (7)	0.0038 (8)	0.0120 (11)	0.0046 (7)
C10	0.2970 (6)	0.4240 (3)	0.0291 (6)	0.0190 (7)	0.0035 (2)	0.0158 (7)	0.0049 (7)	0.0189 (10)	0.0042 (7)
C11	0.5390 (6)	0.2651 (4)	−0.1450 (6)	0.0159 (6)	0.0054 (3)	0.0197 (7)	0.0044 (8)	0.0225 (9)	0.0065 (7)
C12	0.5320 (6)	0.1999 (4)	−0.2963 (6)	0.0205 (8)	0.0058 (3)	0.0169 (7)	0.0061 (9)	0.0221 (10)	0.0052 (8)
C13	0.4313 (6)	0.1076 (4)	−0.3732 (6)	0.0186 (7)	0.0063 (3)	0.0142 (7)	0.0110 (8)	0.0184 (10)	0.0046 (8)
C14	0.3417 (5)	0.0831 (3)	−0.2983 (5)	0.0141 (6)	0.0043 (3)	0.0132 (7)	0.0060 (7)	0.0123 (7)	0.0032 (7)

[a] Numbers in parentheses are estimated standard deviations in the last significant digits. [b] The form of the anisotropic thermal parameter is $\exp[-(\beta_{11}h^2 + \beta_{22}k^2 + \beta_{33}l^2 + \beta_{12}hk + \beta_{13}hl + \beta_{23}kl)]$.

(1)°, $\gamma = 90.01$ (1)°, $V = 947.1$ (3) Å^3, $d_{calcd} = 2.33$ g/cm^3 for $Z = 2$ and a formula weight of 663.41.

A total of 2667 unique reflections with $0° < 2\theta \leq 45°$ were collected using the θ–2θ scan technique, with variable scan rates from 4.0 to 24.0°/min, and a scan range from 2θ (MoKα_1) − 0.9° to 2θ (MoKα_2) + 0.9°. Intensities of three standard reflections measured after every 200 reflections showed no significant variation during data collection. Lorentz and polarization corrections were applied[14] but no absorption correction was made since the average percent transmission was found to be 66 ± 5.

Solution and Refinement of the Structure.[14] The positions of two ruthenium atoms were determined using a three-dimensional Patterson function. These coordinates were refined by two cycles of least-squares refinement to give discrepancy indices of

$$R_1 = (\Sigma\|F_o| - |F_c\|)/\Sigma|F_o| = 0.575$$

$$R_2 = [\Sigma w(|F_o| - |F_c|)^2/\Sigma w|F_o|^2]^{1/2} = 0.616$$

The function, $\Sigma w(|F_o| - |F_c|)^2$, was minimized with the weighting factor, w, equal to $4F_o^2/\sigma(F_o^2)^2$. All structure factor calculations and least-squares refinements were executed using those 2304 reflections for which $F_o^2 > 3\sigma(F_o^2)$. Atomic scattering factors were those of Cromer and Waber.[15] Anomalous dispersion effects were included in the calculated scattering factors for ruthenium.[16]

After both ruthenium atom positions were refined, a difference Fourier map was used to find the third ruthenium atom. The three ruthenium atom positions were refined in three cycles of least-squares refinement to discrepancy factors of $R_1 = 0.265$ and $R_2 = 0.362$. A difference Fourier map now revealed the positions of all remaining nonhydrogen atoms. The positions of all nonhydrogen atoms were refined isotropically by three full-matrix least-squares cycles giving discrepancy factors of $R_1 = 0.61$ and $R_2 = 0.091$. The entire structure was then refined to convergence in four full-matrix least-squares cycles, in which all nonhydrogen atoms were treated anisotropically. The final discrepancy factors were $R_1 = 0.024$ and $R_2 = 0.039$. The error in an observation of unit weight was 0.996. A final difference Fourier map was essentially featureless. A table of observed and calculated structure factor amplitudes is available as supplementary material.

Nuclear Magnetic Resonance Spectra. Enrichment of $(C_4H_4N_2)Ru_3(CO)_{10}$ in ^{13}Co was done in the following manner. A solution of 300 mg of $(C_4H_4N_2)Ru_3(CO)_{10}$ (0.45 mmol) in 100 mL of THF was stirred for 48 h under 150 mL of carbon monoxide enriched to 90% in ^{13}CO. To catalyze the exchange, 10 mg of 10% Pd/activated charcoal was added to the solution. After 48 h the solution was reduced in volume and chromatographed on a short Florisil column, eluting with THF. Final enrichment was approximately 50%. During the exchange there was substantial decomposition to produce $Ru_3(CO)_{12}$.

^{13}C NMR spectra were recorded on a JEOL PS100/Nicolet 1080 Fourier transform NMR spectrometer operating at a frequency of 25.037 MHz. A pulse width of 6 μs, corresponding to a 30° tilt angle, and a repetition time of 1.2 s were employed to collect 2000–4000 scans per spectrum.

Solvents for the variable temperature study were as follows: at 26

Table II. Bond Lengths Å in $(C_4H_4N_2)Ru_3(CO)_{10}$

Ru1–Ru2	2.744 (1)	Ru3–C10	2.219 (6)
Ru2–Ru3	2.861 (1)	N1–N2	1.357 (6)
Ru1–Ru3	2.859 (1)	N1–C11	1.333 (7)
Ru1–N1	2.136 (4)	N2–C14	1.335 (6)
Ru2–N2	2.133 (4)	C11–C12	1.412 (8)
Ru1–C1	1.918 (6)	C13–C14	1.388 (8)
–C2	1.874 (6)	C12–C13	1.375 (8)
Ru2–C3	1.864 (6)	C1–O1	1.143 (7)
–C4	1.899 (6)	C2–O2	1.133 (7)
Ru3–C5	1.944 (6)	C3–O3	1.148 (7)
–C6	1.872 (6)	C4–O4	1.144 (7)
–C7	1.930 (6)	C5–O5	1.114 (7)
Ru1–C8	2.101 (5)	C6–O6	1.151 (7)
Ru2–C8	2.175 (5)	C7–O7	1.152 (7)
Ru2–C9	2.108 (6)	C8–O8	1.160 (6)
Ru3–C9	2.189 (6)	C9–O9	1.152 (7)
Ru1–C10	2.073 (5)	C10–O10	1.151 (7)

[a] Numbers in parentheses are estimated standard deviations in the last significant digits.

Table III. Bond Angles (deg) in $(C_4H_4N_2)Ru_3(CO)_{10}$[a]

Ru2-Ru1-Ru3	61.37 (1)	Ru1-Ru2-C9	110.6 (2)
Ru1-Ru2-Ru3	61.28 (1)	Ru3-Ru2-N2	85.0 (1)
Ru1-Ru3-Ru2	57.35 (1)	-C3	95.3 (2)
Ru2-Ru1-N1	71.0 (1)	-C4	151.6 (2)
-C1	101.6 (2)	-C8	109.0 (1)
-C2	148.4 (2)	-C9	49.5 (2)
-C8	51.3 (1)	N2-Ru2-C3	171.6 (2)
-C10	111.5 (2)	-C4	92.9 (2)
Ru3-Ru1-N1	85.3 (1)	-C8	84.4 (2)
-C1	94.0 (2)	-C9	97.6 (2)
-C2	147.3 (2)	C3-Ru2-C4	90.8 (2)
-C8	111.4 (1)	-C8	87.6 (2)
-C10	50.4 (2)	-C9	88.8 (2)
N1-Ru1-C1	171.9 (2)	C4-Ru2-C8	98.9 (2)
-C2	94.2 (2)	-C9	103.2 (2)
-C8	84.9 (2)	C8-Ru2-C9	157.7 (2)
-C10	96.0 (2)	Ru1-Ru3-C5	94.9 (2)
C1-Ru1-C2	90.8 (2)	-C6	147.5 (2)
-C8	87.9 (2)	-C7	90.9 (2)
-C10	89.6 (2)	-C9	104.3 (2)
C2-Ru1-C8	101.1 (2)	-C10	46.1 (1)
-C10	97.4 (2)	Ru2-Ru3-C5	94.9 (2)
C8-Ru1-C10	161.4 (2)	-C6	155.0 (2)
Ru1-Ru2-N2	71.1 (1)	-C7	91.0 (2)
-C3	101.7 (2)	-C9	47.0 (2)
-C4	144.0 (2)	-C10	103.1 (1)
-C8	48.9 (1)	C5-Ru3-C6	85.8 (2)
C5-Ru3-C7	173.4 (2)	-C6-O6	176.7 (5)
-C9	88.2 (2)	-C7-O7	176.3 (5)
-C10	86.3 (2)	Ru1-C8-O8	142.8 (4)
C6-Ru3-C7	87.5 (2)	Ru2-C8-O8	136.2 (4)
-C9	108.2 (2)	Ru2-C9-O9	141.6 (4)
-C10	101.8 (2)	Ru3-C9-O9	134.9 (4)
C7-Ru3-C9	93.5 (2)	Ru1-C10-O10	144.0 (5)
-C10	95.4 (2)	Ru3-C10-O10	132.5 (5)
C9-Ru3-C10	149.0 (2)	Ru1-N1-N2	108.9 (3)
Ru1-C8-Ru2	79.8 (2)	-C11	130.6 (4)
Ru2-C9-Ru3	83.5 (2)	Ru2-N2-N1	109.0 (3)
Ru1-C10-Ru3	83.5 (2)	-C14	130.8 (4)
Ru1-C1-O1	176.8 (5)	N2-N1-C11	120.5 (4)
Ru1-C2-O2	178.2 (5)	N1-C11-C12	120.8 (5)
Ru2-C3-O3	177.0 (5)	C11-C12-C13	118.3 (6)
Ru2-C4-O4	178.3 (5)	C12-C13-C14	118.5 (5)
Ru3-C5-O5	175.0 (5)	N2-C14-C13	121.7 (5)
		N1-N2-C14	120.2 (4)

[a] Numbers in parentheses are estimated standard deviations in the last significant digits.

and 75 °C, acetone-d_6 and 5% Me_4Si; from −86 to −19 °C, 10% acetone-d_6, 5% Me_4Si, and an equal-volume mixture of C_2H_5Cl and $CFHCl_2$; from −156 to −104 °C, ca. 10% acetone-d_6 and a mixture of CF_2HCl, CF_2Cl_2, $CFHCl_2$, and C_2H_5Cl in approximately the proportions by volume of 45, 20, 15, and 10%. This last mixture was arrived at by trial and error; it gave no viscosity broadening at −156 °C while allowing a relatively high concentration of $(C_4H_4N_2)Ru_3(CO)_{10}$. Approximately 5 mg of $Cr(acac)_3$ was added to each sample. Chemical shifts were measured from internal Me_4Si or the upfield peak of C_2H_5Cl ($\delta_{C_2H_5Cl} = \delta_{Me_4Si} + 19.2$ ppm). Chemical shifts in Figure 2 are as follows: A = 202.4, B = 201.6, C = 200.4, D = 198.6, E = 196.2, F = 262.3, G = 256.7 ppm. The value of J_{C-Ru-C} (trans) in the B and E resonances is 36 ± 2 Hz.

The NMR spectra were computer simulated using the program EXCHSYS by G. M. Whitesides and J. K. Krieger. The exchange process involving resonances C, D, F, and G in the temperature range −156 to −104 °C were simulated assuming an ab_2cd_2 system. The general exchange processes occurring in the temperature range −34 to 75 °C were simulated assuming an a_7b_2c system. Calculations were performed at close τ intervals over the exchange region for a good fit for kinetic analysis.

Results

Molecular Structure in the Crystal. The molecular structure is shown in Figure 1, where the numbering scheme is defined.

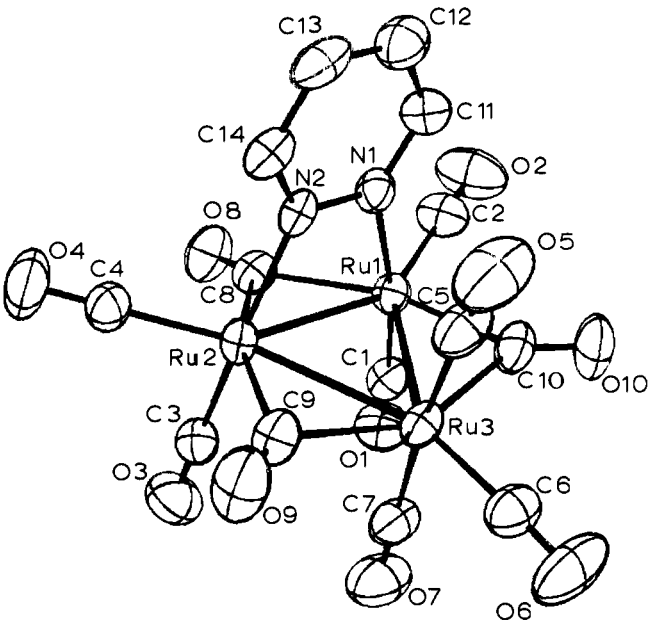

Figure 1. The molecular structure of $Ru_3(C_4H_4N_2)(CO)_{10}$. Each atom is represented by its ellipsoid of thermal vibration scaled to enclose 50% of its electron density. The numbering scheme employed in Tables I–III is defined.

Tables I–III record atomic positional and thermal parameters, bond lengths, and bond angles, respectively. While there is no crystallographically required symmetry, the molecule has a virtual plane of symmetry passing through Ru(3) and its three CO ligands, through the bridging C(8)-O(8) group and bisecting, inter alia, the N-N bond.

The Ru-Ru bond lengths here are of two types. The one that is bridged by $C_4H_4N_2$ as well as by a CO group is unusually short, 2.744 Å, while the other two, 2.861 (1) and 2.859 (1) Å, are slightly long, when compared to the average Ru-Ru distance in $Ru_3(CO)_{12}$, namely, 2.848 Å.[4]

The Ru-C distances for the bridging CO groups vary from 2.073 (5) Å to 2.219 (6) Å. Some of these variations conform to the virtual minor symmetry, but some do not. Thus, the two Ru(3)-C(br) distances are the two longest ones, 2.189 (6) and 2.219 (6) Å, and they differ by a little less than three times the sum of their esd's. They are, in effect essentially equal with an average value of $2.220_5 \pm 0.01_5$ Å. The next mirror-related pair, Ru(1)-C(10) = 2.073 (5) Å and Ru(2)-C(9) = 2.108 (6) Å, are also little different from each other, with an average value of $2.09_0 \pm 0.01_8$ Å. The difference between these two averages is certainly real, i.e., statistically significant, and presumably reflects the different electron densities at Ru(3) on the one hand and Ru(1) and Ru(2) on the other. The third bridging CO group is also somewhat unsymmetrical, with the two Ru-C distances differing by 0.074 Å, but this is presumably a packing distortion having no chemical significance.

The Ru-C distances for the terminal CO groups vary from 1.864 Å to 1.944 Å, but there does not appear to be any pattern having chemical significance except that those on Ru(3), where all ligands are CO groups, have a higher average value, 1.915 Å, than those on Ru(1) and Ru(2), for which the average is 1.888 Å. This difference, while barely significant, does correspond with the expectation that CO groups on Ru(1) and Ru(2) would be shorter because they should be more strongly π bonded to the metal atoms than those on Ru(3). No useful comparison with values for $Ru_3(CO)_{12}$ itself is possible owing to the low accuracy of those values and the large scatter in both sets.

The $C_4H_4N_2$ ligand forms bonds of equal lengths to each Ru atom. In this case, compared to $C_4H_4N_2Fe_2(CO)_7$,[17] the

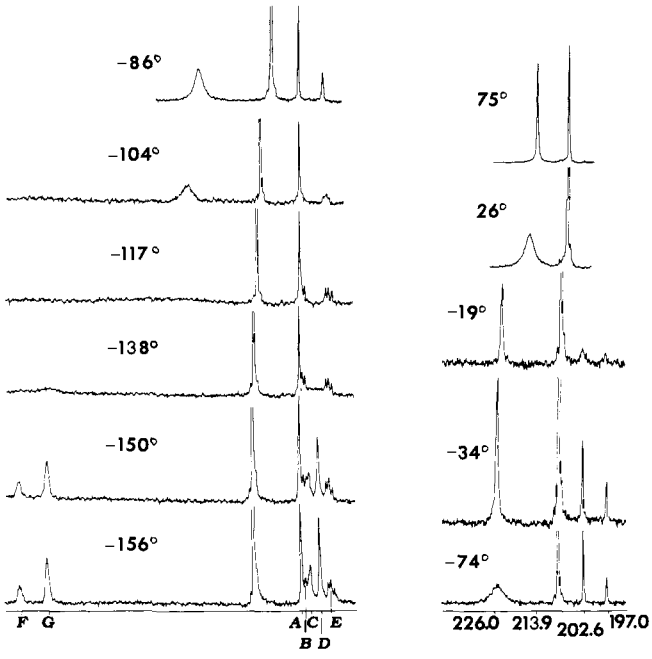

Figure 2. Carbon-13 nuclear magnetic resonance spectra for $(C_4H_4N_2)Ru_3(CO)_{10}$. Chemical shifts (lower right) are in parts per million downfield from Me_4Si.

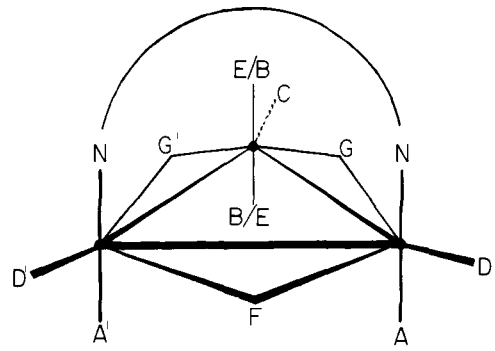

Figure 3. A schematic representation of the structure of $(C_4H_4N_2)Ru_3(CO)_{10}$, labeled in accord with the assignment proposed in the text.

alternation in C–C and C–N distances around the ring is a little more noticeable, but it is unlikely that any important degree of π-bond localization is indicated.

Stereodynamic Behavior. The spectral changes as a function of temperature that form the basis for discussion are displayed in Figure 2. Our first task is to present an interpretation of these spectra. Clearly, the spectrum at −156 °C is in accord with the structure seen in the crystal, and it may safely be concluded that this is, indeed, the instantaneous structure of the molecule in solution. The proposed assignment of the spectrum is indicated by comparing the capital letters A–G under the −156 °C spectrum with the carbonyl labeling scheme shown in Figure 3.

The two downfield signals must be due to the bridging CO's, F, G, and G′. The validity of the remaining assignments is not evident solely from the characteristics of the −156 °C spectrum itself but arises from other considerations, including the changes that occur between −156 and −86 °C.

In this temperature range, it is clear that signals C, D, F, and G broaden, and disappear, while a new peak of intensity comparable to the total intensity of those which have disappeared forms at approximately the average of their original positions. Clearly the three bridging CO groups are scrambling with three terminal CO groups, and we identify the latter as the equatorial ones. The only possible alternative would be to select those labeled A, A′, and one of the axial CO's on the unique metal atom. However, this last possibility must be rejected in order to explain the persistence of ^{13}C–^{13}C coupling on two of the remaining signals, i.e., those labeled B and E. Only two CO groups on the same metal atom can satisfy this requirement, and, moreover, only the two which are trans to each other. There is no sure way to decide which of these two carbonyl groups, B and E, gives rise to which signal. The possibility of leaving carbonyl group C and *one* of the axial CO's fixed at this stage requires the assumption that the observed coupling is between these two cis CO groups. If this were true, then in the slow exchange spectrum we should have to see *three* signals each of relative intensity 1 split up by ^{13}C–^{13}C coupling, and this is not what we observe.

Thus, there is a well-defined first stage of fluxionality in which the six CO groups that are approximately coplanar with the Ru_3 triangle are scrambled.

A second stage of fluxionality is observed between about −117 and −86 °C. The ^{13}C–^{13}C spin–spin splitting of resonance E is abolished while simultaneously resonance B disappears. It is certain that resonance B merges with the broad low-field signal because during the same temperature range as resonance B disappears the broad low-field resonance (a) shifts approximately $\frac{1}{7}$ of the distance between its initial position and that of distance between its initial position and that of resonance B, and (b) first increases its width and then again narrows (compare the −86, −74, and −34 °C spectra). Thus, one of the axial CO groups on Ru(3) is entering into the scrambling process already occurring rapidly among the equatorial CO groups. The other axial CO group on Ru(3) remains fixed but becomes decoupled from the other one because the other one is no longer fixed in the trans position.

A third and final stage of fluxionality becomes observable above −34 °C. In this stage all three of the separate resonances, of relative intensities 7 (B, C, D, C′, F, G, G′), 2 (A, A′), and 1 (E), coalesce to one signal which is fully sharpened, or very nearly so, at 75 °C.

By the usual process of fitting computed spectra for various mean residence times to observed spectra, the activation parameters for the first and third fluxional processes have been evaluated and are presented in Table IV.

Discussion

The observation of a structure with only three equatorial terminal CO groups and three bridging ones, in contrast to the structure of $Ru_3(CO)_{12}$ itself, where all equatorial CO groups are terminal, is important in suggesting that the two arrangements differ little in energy. By a relatively small manipulation of the electron density distribution, attendant upon replacing two cis axial CO groups by two amine nitrogen atoms, the preferred arrangement of the six equatorial CO groups has been changed from one of the two symmetrical limiting arrangements to the other. Since each of these arrangements constitutes an intermediate between two permutamers of the other type, it is clear that if there is only a small (i.e., <20 kcal) energy difference between the two types, a special form of partial CO scrambling becomes possible. In this process the six equatorial CO groups will move around the central Ru_3 triangle, passing from one metal atom to another but always preserving their initial cyclic order.

As mentioned in the introduction, and noted explicitly in an earlier publication from this laboratory,[2] this would be an unperceived or hidden process in the parent molecule since in the slow exchange limit of general (i.e., axial as well as equatorial) scrambling, such a cycling of the equatorial CO groups could continue, rapidly, without any effect on the spectral line shapes in molecules of normal isotopic composition. Even in

Table IV. Activation Parameters for $(C_4H_4N_2)Ru_3(CO)_{10}$

	E_a, kcal mol^{-1}	Log A	$\Delta G^{\ddagger}$, kcal mol^{-1}	$\Delta H^{\ddagger}$, kcal mol^{-1}	$\Delta S^{\ddagger}$, eu
In-plane scrambling	6.1 (1)	12.4 (2)	6.5 (1)	5.8 (1)	−2.4 (5)
General scrambling	13.9 (2)	13.9 (3)	12.4 (2)	13.3 (2)	3.0 (5)

molecules enriched in ^{13}C, there would be no observable effect if the ^{13}C–^{13}C coupling constant between axial and equatorial CO groups on the same metal atom has a negligible value, as appears to be the case.

In this investigation we have designed, built, and stereodynamically characterized a derivative of $Ru_3(CO)_{12}$ capable of revealing the existence of the otherwise "unperceived" process of in-plane cycling of equatorial ligands. The most prominent and important result of our work is that the existence of such a process has been demonstrated. In this particular case it is an exceptionally facile process, with an activation energy of only about 6 kcal mol^{-1} (Table IV) and only at about the lower practical limit of experimentation could a slow-exchange spectrum be observed.

Two further fluxional processes come into play as the temperature is raised, but for neither of these does any particular pathway for scrambling uniquely suggest itself. In fact, for the process whose effects are seen in the spectra at −104, −86, and −74 °C, in which one of the two axial CO groups, B or E, joins in the already rapid in-plane scrambling, we cannot even determine with certainty which of the two CO groups (see Figure 3) is participating. The assignment of resonance B to the CO group on the opposite side of the Ru_3 plane from the 1,2-diazine ring on the grounds that the ring current effect of the diazine should move the other axial CO group (which gives signal E) upfield has some merit but is inconclusive. It is really the *difference* in the environments of the two axial CO groups on Ru(3) that matters and thus the diamagnetic anisotropy of the CO groups A and A′ must also be considered. We are not certain how to evaluate that and thus we take the position that assignment of resonances B and E might be made in either of the two ways implied by Figure 3, in the absence of further data.

The final stage of scrambling, in which all signals coalesce into one, clearly involves the passage of all CO groups over all seven structurally distinct sites. This follows from the fact that the equatorial CO groups are already rapidly passing over the four in-plane sites and from one metal atom to another. The axial CO groups, as they are exchanged with those in the set of six equatorial ones, will necessarily be carried from one metal atom to another and hence over all the axial sites as well as over all the equatorial ones, while any initially equatorial group will sooner or later get to each of the axial sites.

There is simply no basis on which to choose any particular process—or processes—for exchanging axial and equatorial CO groups. If the intermediate stage of the in-plane cycling process, in which all equatorial CO groups are terminal, is a structure of sufficient lifetime, the kind of process depicted in Scheme I, and already discussed for $Ru_3(CO)_{12}$ itself,[10] is an attractive possibility.

The fluxional behavior observed here has interesting parallels to the behavior of $(C_4H_4N_2)Fe_2(CO)_7$, in which there are two stages of fluxional behavior.[17] In the first stages five essentially coplanar ligands, four terminal and one bridging, are scrambled, presumably in a cyclic process, while two axial CO groups remain separate. Then, at higher temperature the two axial groups also enter into a general scrambling process.

The final point we wish to note here has to do with the bearing of the present results on the validity of the totally "concerted" process proposed by Johnson[3] for CO scrambling in $Fe_3(CO)_{12}$. Johnson, following up his earlier suggestions[18] attributing a preeminent role to repulsions between CO groups in determining the structures of di- and polynuclear metal carbonyl compounds,[19] has proposed that for $Fe_3(CO)_{12}$ the CO groups preserve a fixed, hollow icosahedral arrangement while the Fe_3 triangle rotates within, thus allowing all CO groups to scramble over the distinguishable types of sites.

Presumably this idea of a metal atom cluster rotating within the shell of ligands is more generally applicable (if it is applicable at all). In addition, it seems to us that the replacement of two CO groups by $C_4H_4N_2$ should not invalidate the premises of Johnson's suggestion, assuming that these premises are valid to begin with. Thus, again, movement of the triangle of metal atoms within a relatively rigid "exoskeleton" of ligands might be expected. The observations, however, are not consistent with this. If the triangle of metal atoms were to rotate in the equatorial plane while the ligand set remained fixed, the C, D, F, and G resonances would *not* coalesce. Only by motion of the set of equatorial CO groups relative to *all of the other atoms* can the observed spectral changes be accounted for. In other words, the ligand atoms do not preserve a fixed spatial arrangement among themselves; on the contrary, some of them move relative to others.

It is perhaps pertinent to note that even in the case of $Os_6(CO)_{18}$, that is, in a case where all the ligands are CO groups, *only* processes in which *selected* sets of CO groups are scrambled have been observed[20] while no scrambling of the sort that would result from motion of the Os_6 unit as a whole relative to the ligand set as a whole has been seen.

Acknowledgment. We thank the Robert A. Welch Foundation for support under Grant A494. J.D.J. was a Robert A. Welch Postdoctoral Fellow during 1975-1976.

Supplementary Material Available: A table of observed and calculated structure factor amplitudes (10 pages). Ordering information is given on any current masthead page.

References and Notes

(1) (a) J. Lewis and B. F. G. Johnson, *Pure Appl. Chem.*, **44**, 43 (1975), especially pp 63–76; (b) O. Gambino, M. Valle, S. Aime, and G. A. Vaglio, *Inorg. Chim. Acta*, **8**, 71 (1974); (c) A. J. Deeming and M. Underhill, *J. Chem. Soc., Dalton Trans.*, 2727 (1973); (d) T. H. Whitesides and R. A. Budnick, *J. Chem. Soc., Chem. Commun.*, 87 (1973).
(2) F. A. Cotton and J. D. Jamerson, *J. Am. Chem. Soc.*, **98**, 5396 (1976).
(3) B. F. G. Johnson, *J. Chem. Soc., Chem. Commun.*, 703 (1976).
(4) (a) C. H. Wei and L. F. Dahl, *J. Am. Chem. Soc.*, **91**, 1351 (1969); (b) F. A. Cotton and J. M. Troup, *ibid.*, **96**, 4155 (1974).
(5) R. Mason and A. I. M. Rae, *J. Chem. Soc. A*, 788 (1968).
(6) E. R. Corey and L. F. Dahl, *Inorg. Chem.*, 1, 521 (1962).
(7) F. A. Cotton, *Prog. Inorg. Chem.*, **21**, 1 (1976), and primary references cited therein.
(8) F. A. Cotton and D. L. Hunter, *Inorg. Chim. Acta*, **11**, L9 (1974).
(9) L. J. Todd and J. R. Wilkinson, *J. Organomet. Chem.*, **77**, 1 (1974).
(10) A. Forster, B. F. G. Johnson, J. Lewis, T. W. Matheson, B. H. Robinson, and G. W. Jackson, *J. Chem. Soc., Chem. Commun.*, 1042 (1974).
(11) L. Milone, S. Aime, E. W. Randall, and E. Rosenberg, *J. Chem. Soc., Chem. Commun.*, 452 (1975).
(12) B. F. G. Johnson, J. Lewis, B. E. Reichert, and K. T. Schorpp, *J. Chem. Soc., Chem. Commun.*, 1403 (1976).
(13) F. A. Cotton, B. A. Frenz, G. Deganello, and A. Shaver, *J. Organomet. Chem.*, **50**, 227 (1973).
(14) Computer programs used were those of the Enraf-Nonius Structure Determination Package on the PDP 11/45 computer system at the Molecular Structure Corp., College Station, Texas.
(15) D. T. Cromer and J. T. Waber, "International Tables for X-Ray Crystallography", Vol. IV, Kynoch Press, Birmingham, England, 1974, Table 2.3.1.
(16) D. T. Cromer and D. Liberman, *J. Chem. Phys.*, **53**, 1891 (1971).
(17) F. A. Cotton, B. E. Hanson, J. D. Jamerson, and B. R. Stults, *J. Am. Chem.*

Soc., 99, 3293 (1977).
(18) B. F. G. Johnson, J. Chem. Soc., Chem. Commun., 211 (1976).
(19) It has been argued that Johnson's concept cannot be supported by quantitative calculations which suggest instead that the traditional view in which nonbonded repulsions are only one of a number of forces, the others being those of directed valence, may not yet need to be abandoned. Cf. P. B. Hitchcock, R. Mason, and M. Textor, J. Chem. Soc., Chem. Commun., 1047 (1976).
(20) C. R. Eady, W. G. Jackson, B. F. G. Johnson, J. Lewis, and T. W. Matheson, J. Chem. Soc., Chem. Commun., 958 (1975).

Effects of Para Substituent and Metal Ion on Rates of Phenyl Ring Rotation in Ruthenium, Indium, and Titanium Complexes of Para-Substituted Tetraphenylporphyrins

S. S. Eaton* and G. R. Eaton

Contribution from the Departments of Chemistry, University of Colorado at Denver, Denver, Colorado 80202, and University of Denver, Denver, Colorado 80208.
Received April 22, 1977

Abstract: Rates of phenyl ring rotation in para-substituted tetraphenylporphyrin complexes with ruthenium carbonyl 4-*tert*-butylpyridine, indium chloro, and titanyl ions were studied by variable temperature ^{1}H NMR of the phenyl resonances. Para substituents examined were trifluoromethyl, chloro, methyl, isopropyl, methoxy, and diethylamino (ruthenium, indium, titanyl) and hydroxy (titanyl). Activation parameters obtained by total line shape analysis are in the ranges $\Delta G^{\ddagger}_{298}$ = 14.3–18.6 kcal/mol, $\Delta H^{\ddagger}$ = 11.2–17.5 kcal/mol, and $\Delta S^{\ddagger}$ = −3.7 to −12.4 eu. Rates as a function of metal ion increase in the order ruthenium < indium < titanyl. Rates are faster for electron-donating substituents than for electron-withdrawing subsituents, but do not give a linear correlation with Hammett σ_p values.

Rotation of phenyl rings in tetraphenylporphyrin complexes of Ru,[1-4] Ge,[5] Ti,[3,4,6] In,[3,4,7] and Fe[8] has been reported. Phenyl ring substituents have recently been shown to influence rates of copper ion incorporation,[9] rates of inversion of ferric porphyrins,[10] rates of axial ligand exchange in ruthenium carbonyl porphyrins,[11] basicity and electronic spectra of free porphyrins,[9,12] equilibrium constants for axial ligation in $(VO)^{2+}$,[13] Fe,[14,15] Co,[16] Ni,[13] and Zn[17] porphyrins, and redox potentials of free porphyrins,[18,19] Co,[16,19] Fe,[20] and Ni[21] porphyrins. A previous paper in this series demonstrated that the dynamic process observed in the ^{1}H NMR of the phenyl resonances of ruthenium carbonyl, indium chloro, and titanyl complexes of para-substituted tetraphenylporphyrins was due to phenyl ring rotation.[4] This report concerns the effect of para substituents and metal ion on the rate of the phenyl ring rotation for an extended series of para substituents for these metals, and includes activation parameters obtained by total line shape analysis.

Experimental Section

Physical Measurements. Infrared spectra were recorded as Nujol or halocarbon mulls on Perkin-Elmer 710 or 337 grating spectrometers. Visible spectra were obtained in chloroform solutions on a Beckman Acta V spectrometer. Data are given below with wavelengths in nanometers and log ϵ in parentheses. ^{1}H NMR spectra were run at power levels well below saturation on a Varian HA-100 spectrometer equipped with a variable-temperature probe. Spectra were obtained with the spectrometer locked on the solvent resonance (1,1,2,2-tetrachloroethane). ^{1}H NMR chemical shifts were measured with respect to 1,1,2,2-tetrachloroethane ($C_2H_2Cl_4$) and are reported below in parts per million downfield of Me_4Si using a correction of 5.96 ppm for the chemical shift of 1,1,2,2-tetrachloroethane at ca. 32 °C.

Preparation of Compounds. The following compounds were prepared and characterized by literature methods: Ru(CO)(*p*-R-TPP)(*t*-Bupy),[22] R = CF_3, Cl, Me, OMe, Et_2N;[11] Ru(CO)(*p*-*i*-Pr-TPP)(*t*-Bupy);[1] TiO(*p*-R-TPP), R = CF_3, *i*-Pr;[4] In(*p*-R-TPP)Cl, R = CF_3, *i*-Pr;[4] In(*p*-R-TPP)Cl, R = Me, OMe;[23] H_2(*p*-CF_3-TPP);[4] H_2(*p*-R-TPP), R = Cl, Me, OMe;[24,25] H_2(*p*-*i*-Pr-TPP);[1] H_2(*p*-Et_2N-TPP).[26] All chromatography was on Baker 0537 alumina.

TiO(*p*-R-TPP), R = Cl, Me, OMe, Et_2N. These compounds were prepared by the method reported for TiO(octaethylporphyrin).[27] Crude complexes were chromatographed on alumina and recrystallized from dichloromethane/hexane. Details of chromatography conditions, yield, and characterization data are given below for individual complexes.

TiO(*p*-Cl-TPP). Chromatography. The crude product was put on a column in benzene. Free porphyrin was eluted with benzene and the complex eluted with 1:1 CH_2Cl_2–benzene: yield 91%; IR ν_{TiO} 840 cm^{-1}; visible spectrum 403 sh (4.62), 424 (5.69), 514 (3.49), 552 (4.40), 590 nm (3.56); ^{1}H NMR (0 °C) pyrrole H, 9.18 (singlet), *o*-H, 8.44, 8.05 (doublets), *m*-H, 7.87, 7.77 ppm (doublets). Anal. Calcd for $C_{44}H_{24}N_4Cl_4TiO$: C, 64.89; H, 2.97; N, 6.88; Cl, 17.41. Found: C, 64.77; H, 3.24; N, 6.88; Cl, 17.21.

TiO(*p*-Me-TPP). Chromatography. The crude complex was put on a column in trichloroethylene (C_2HCl_3). Free porphyrin was eluted with C_2HCl_3 and the complex eluted with 1:1 C_2HCl_3–$CHCl_3$: yield 57%; IR ν_{TiO} 975 cm^{-1}; visible spectrum 406 sh (4.61), 426 (5.70), 516 (3.51), 553 (4.40), 5.92 nm (3.75); ^{1}H NMR (0 °C) pyrrole H, 9.22 (singlet), *o*-H, 8.40, 8.00 (doublets), *m*-H, 7.68, 7.57 (doublets), CH_3, 2.74 ppm (singlet). Anal. Calcd for $C_{48}H_{36}N_4TiO$: C, 78.68; H, 4.95; N, 7.65. Found: C, 78.56; H, 5.08; N, 7.98.

TiO(*p*-OMe-TPP). Chromatography. The crude complex was put on a column in benzene. Free porphyrin was eluted with benzene and the complex eluted with 1:1 CH_2Cl_2–benzene: yield 58%; IR ν_{TiO} 970 cm^{-1}; visible spectrum 408 sh (4.63), 429 (5.62), 517 (3.51), 554 (4.34), 596 nm (3.88); ^{1}H NMR (0 °C) pyrrole H, 9.19 (singlet), *o*-H, 8.42, 8.03 (doublets), *m*-H, 7.39, 7.28 (doublets), CH_3, 4.12 (singlet). These values are in good agreement with those published for an alternate preparation of the compound.[6] Anal. Calcd for $C_{48}H_{36}N_4TiO_5$: C, 72.36; H, 4.55; N, 7.03. Found: C, 72.39; H, 4.26; N, 7.05.

TiO(*p*-Et_2N-TPP). The reaction time was shortened to 1 h and the diethylene glycol was removed by extraction from a chloroform solution of the product into 1:1 methyl ethyl ketone–H_2O. The crude product was put on a column in benzene. Free porphyrin was eluted with benzene and the product eluted with 1:1 $CHCl_3$–benzene: yield 64%; IR ν_{TiO} 975 cm^{-1}; visible spectrum 398 (4.80), 460 (5.17), 568